Supplementary Information

H3K9 methylation drives resistance to androgen receptor–antagonist therapy in prostate cancer

One sentence summary: H3K9me3 enables antiandrogen resistance.

Mehdi Baratchian[1,+], Ritika Tiwari[1,+], Sirvan Khalighi[2], Ankur Chakravarthy[3], Wei Yuan[5], Michael Berk[1], Jianneng Li[1], Amy Guerinot[1], Johann de Bono[5], Vladimir Makarov[6], Timothy A. Chan[6], Robert H. Silverman[7], George R. Stark[7], Vinay Varadan[2], Daniel D. De Carvalho[3,4], Abhishek A. Chakraborty[1], Nima Sharifi[1,7,8,9 *]

[1]Genitourinary Malignancies Research Center, Lerner Research Institute, Cleveland Clinic, Cleveland, USA.

[2]Case Comprehensive Cancer Center, Case Western Reserve University, Cleveland, USA.

[3]Princess Margaret Cancer Centre, University Health Network, Toronto, Ontario, Canada.

[4]Department of Medical Biophysics, University of Toronto, Toronto, Ontario, Canada.

[5]Division of Clinical Studies, The Institute of Cancer Research and Royal Marsden Hospital, London, UK.

[6]Center for Immunotherapy and Precision Immuno-Oncology, Lerner Research Institute, Cleveland Clinic, Cleveland, USA.

[7]Department of Cancer Biology, Lerner Research Institute, Cleveland Clinic, Cleveland, USA.

[8]Department of Hematology and Oncology, Taussig Cancer Institute, Cleveland Clinic, Cleveland, USA.

[9]Department of Urology, Glickman Urological and Kidney Institute, Cleveland Clinic, Cleveland, USA.

[+]Denotes equal contribution; *Corresponding author: sharifn@ccf.org;

Supplementary Figures

Figure S1

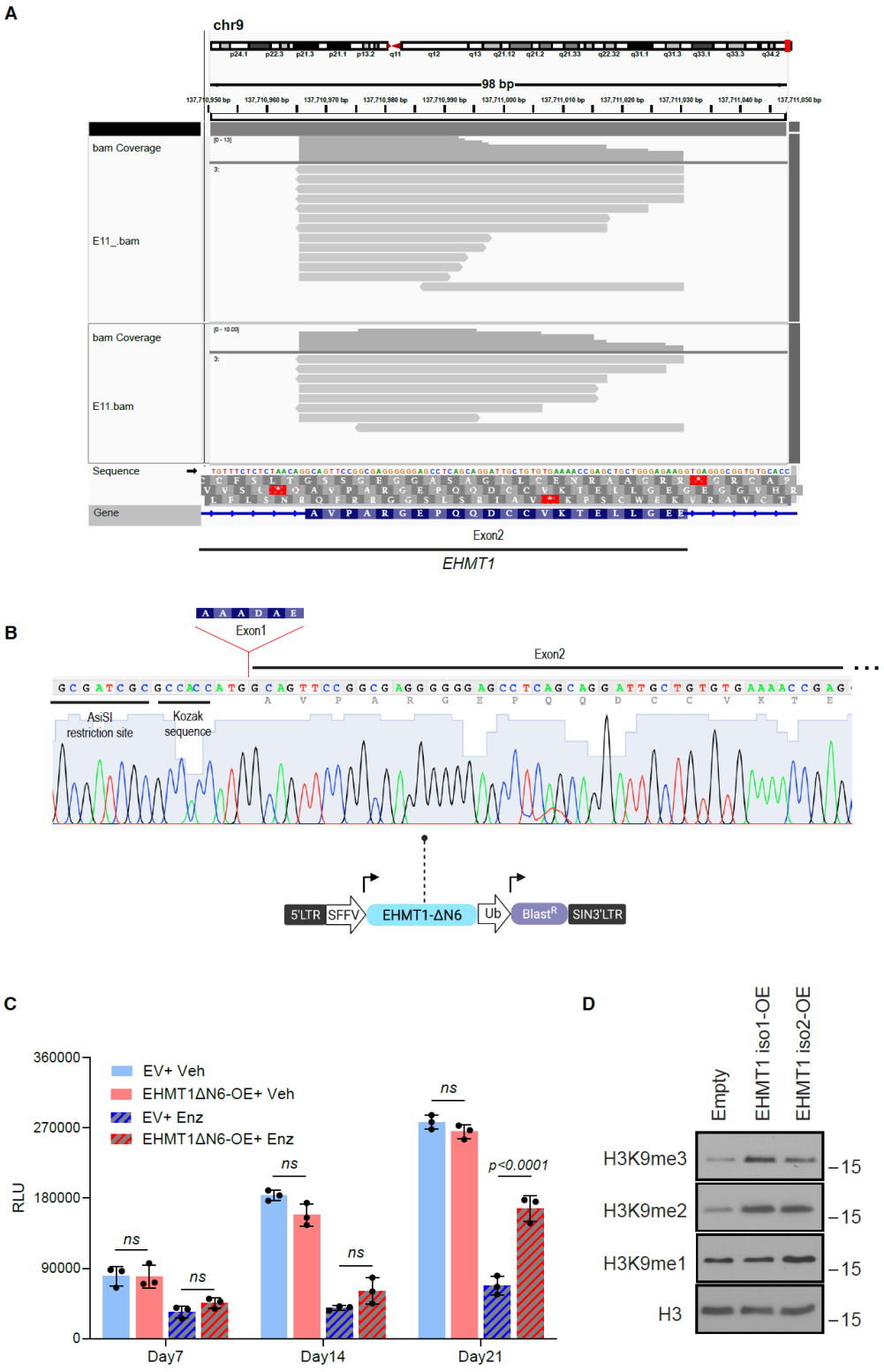

Figure S1. Forward genetic screen identified EHMT1 as a crucial mediator of enzalutamide resistance in prostate cancer. A) Graphical representation of the VBIM integration site into the EHMT1 gene. VBIM-tagged transcripts were first selected using a 50nt barcode and then aligned to the human genome hg.38. The integrative genomics viewer (IGV) snapshot shows that the identified VBIM-tagged reads mapped to the first codon of exon 2 of the EHMT1 isoform1 excluding only the 6 N-terminal amino acids of the protein that belong to exon 1. B) Schematic representation of the overexpression lentiviral construct encoding EHMT1 lacking the first 6 N-terminal aa (EHMT1ΔN6). C) Cell growth analysis of LNCaP cells lentiviral transduced with empty vector (EV) or EHMT1ΔN6 construct, followed by treatment with vehicle or Enz (10μM) for 21 days. The differences in cell growth were determined by CellTiter-Glo luminescent cell viability assay. D) Immunoblots showing the expression of indicated histones in lentivirally transduced LNCaP cells overexpressing control, EHMT1iso1 and EHMT1iso2 constructs. Total Histone H3 was used as a loading control.

Figure S2

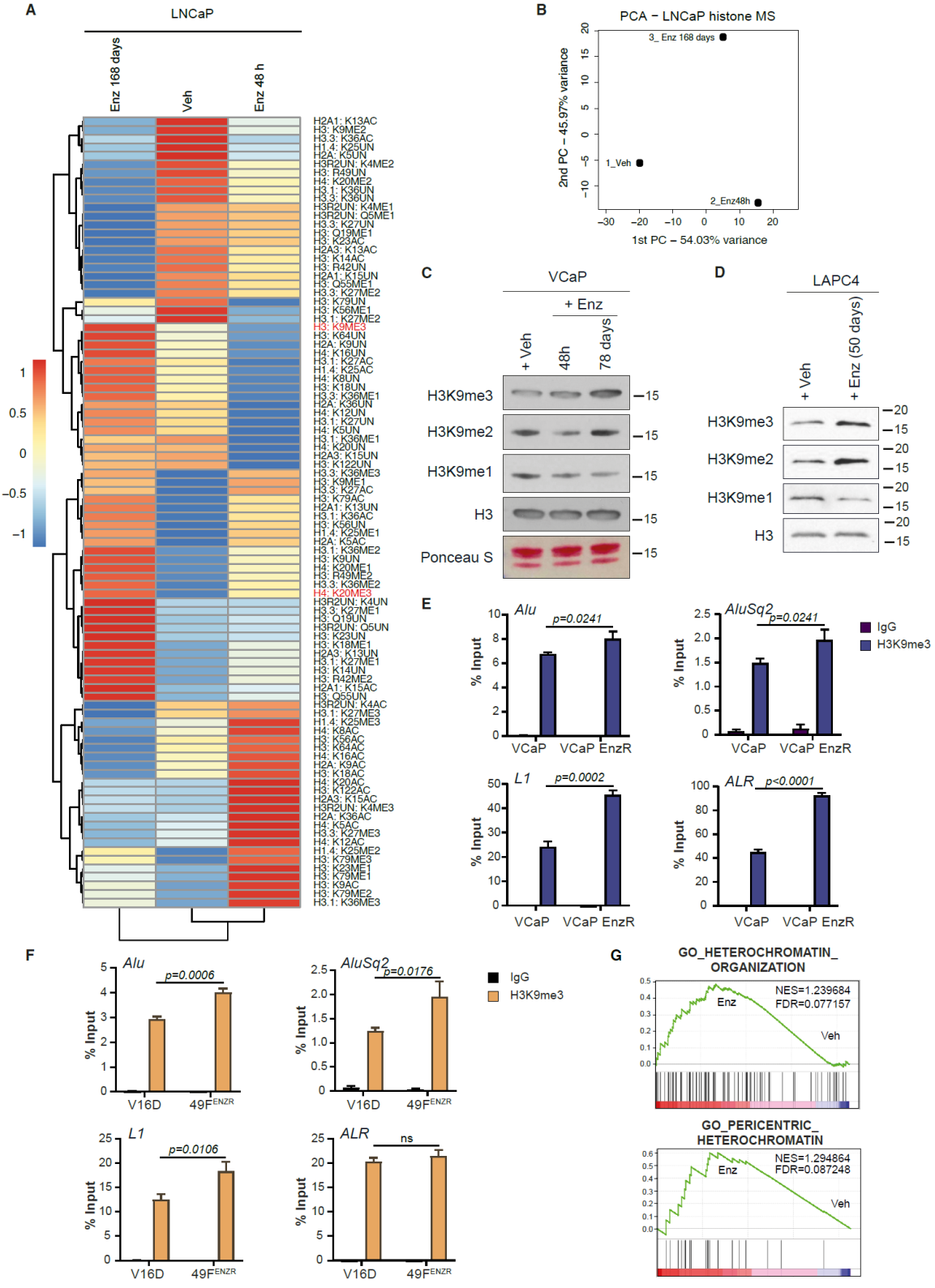
A
LNCaP
Enz 168 days
Veh
Enz 48 h
B
PCA – LNCaP histone MS
3_ Enz 168 days
1_Veh
2_Enz48h
2nd PC – 45.97% variance
1st PC – 54.03% variance
C
VCaP
+ Enz
+ Veh
48h
78 days
H3K9me3
H3K9me2
H3K9me1
H3
Ponceau S
D
LAPC4
+ Veh
+ Enz (50 days)
H3K9me3
H3K9me2
H3K9me1
H3
E
Alu
AluSq2
L1
ALR
p=0.0241
p=0.0241
p=0.0002
p<0.0001
% Input
VCaP
VCaP EnzR
IgG
H3K9me3
F
Alu
AluSq2
L1
ALR
p=0.0006
p=0.0176
p=0.0106
ns
% Input
V16D
49F ENZR
IgG
H3K9me3
G
GO_HETEROCHROMATIN_ ORGANIZATION
NES=1.239684
FDR=0.077157
Enz
Veh
GO_PERICENTRIC_ HETEROCHROMATIN
NES=1.294864
FDR=0.087248
Enz
Veh

Figure S2. Chronic Enz treatment leads to accumulation of H3K9me3 in prostate cancer cell line models. A) Heatmap representing relative abundance of histone modifications determined by mass spectrometry in LNCaP cells treated with DMSO (Veh) or Enz (10 μM) for 48 hours or 168 days. The color in each cell represents z-score derived from relative abundance of each modification across samples, measured in three technical replicates. B) Principal component analysis (PCA) showing separation of samples described in (B) based on the first principal components. C) Immunoblot analysis of H3K9 methylation marks on histone extracts purified from VCaP cells treated with vehicle or Enz (1μM) for 48 hours or 78 days. D) Histone immunoblot analysis on whole cell extracts from LAPC4 cells treated with vehicle or Enz (10μM) for 50 days. E) ChIP-qPCR analysis of H3K9me3 levels at the indicated REs in VCaP versus VCaP EnzR cells. F) Same as E except V16D versus 49F^{ENZR} cells were used. V16D is an enzalutamide sensitive CRPC cell line developed from LNCaP cells and its derivative cell line, 49F^{ENZR} was developed by multiple serial transplantation of the enzalutamide-resistant tumors in athymic male mice. G) GSEA plots showing gene signatures associated with heterochromatin along with corresponding statistical metrics in LNCaP cells treated with Enz (10μM) versus DMSO (Veh) for 84 days.

Figure S3

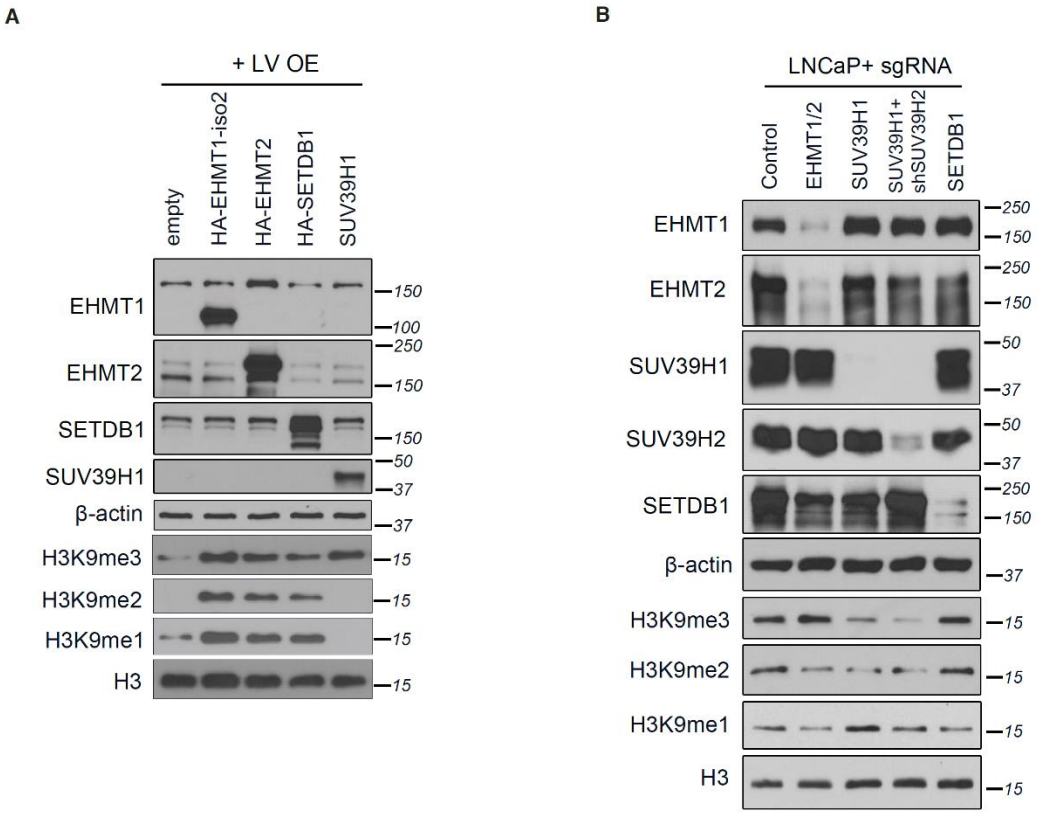

Figure S3. Modulating the expression of H3K9 methyltransferases affects the global levels of H3K9 methylation. A) Immunoblots showing the expression of ectopically expressed H3K9 methyltransferases and H3K9 methylation marks in LNCaP cells. B) Immunoblots showing the expression of H3K9 methyltransferases and H3K9 methylation marks in LNCaP cells lentivirally transduced with guide RNAs or shRNA targeting the indicated H3K9 methyltransferase, or a non-targeting control gRNA.

Figure S4

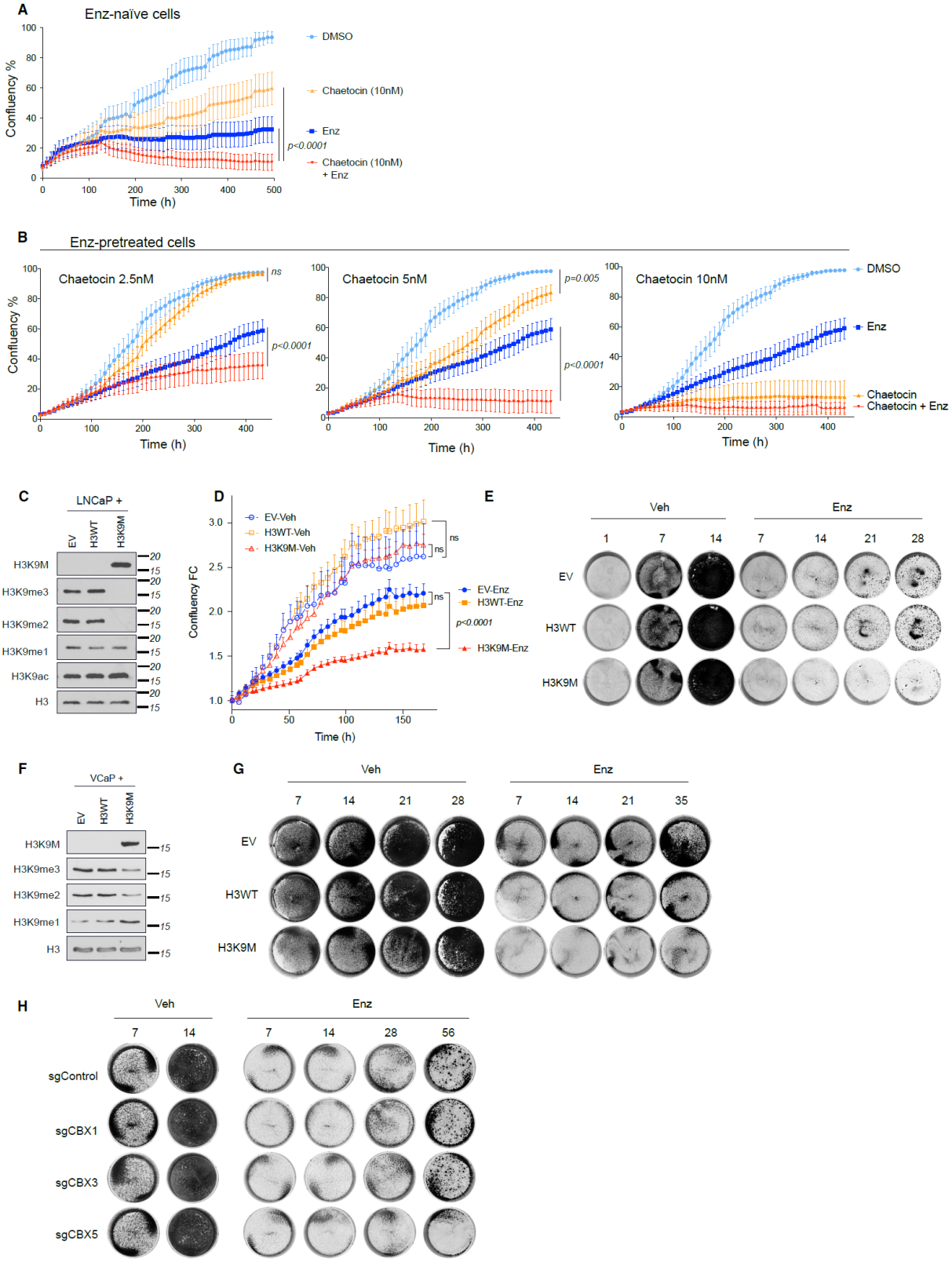
A
Enz-naïve cells
Confluency %
Time (h)
DMSO
Chaetocin (10nM)
Enz
p<0.0001
Chaetocin (10nM) + Enz
B
Enz-pretreated cells
Chaetocin 2.5nM
Chaetocin 5nM
Chaetocin 10nM
ns
p<0.0001
p=0.005
p<0.0001
DMSO
Enz
Chaetocin
Chaetocin + Enz
C
LNCaP +
EV
H3WT
H3K9M
H3K9M
H3K9me3
H3K9me2
H3K9me1
H3K9ac
H3
D
EV-Veh
H3WT-Veh
H3K9M-Veh
Confluency FC
Time (h)
ns
ns
ns
EV-Enz
H3WT-Enz
p<0.0001
H3K9M-Enz
E
Veh
Enz
1
7
14
7
14
21
28
EV
H3WT
H3K9M
F
VCaP +
EV
H3WT
H3K9M
H3K9M
H3K9me3
H3K9me2
H3K9me1
H3
G
Veh
Enz
7
14
21
28
7
14
21
35
EV
H3WT
H3K9M
H
Veh
Enz
7
14
7
14
28
56
sgControl
sgCBX1
sgCBX3
sgCBX5

Figure S4. Genetic or pharmacologic inhibition of H3K9 tri-methylation strongly sensitizes cells to Enz. A-B) Cell growth analysis of LNCaP cells treated with DMSO (Veh) or chaetocin (25, 50 and 100nM) for 72 hours by IncuCyte live cell monitoring in Enz-naïve or Enz-pretreated LNCaP cells treated with Veh or Enz (10μM). Statistical differences between groups were determined by unpaired *t*-test and error bars represent SEM. Cells in (B) were pretreated with Enz (10μM) for 90 days before initiation of the experiment. C-E) Immunoblots (C), cell growth as monitored by IncuCyte live cell imaging (D), and representative crystal violet stained images (E) of of LNCaP cells that were lentivirally transduced to express empty vector, H3.1WT, or H3.1K9M. Data in (D) represent mean ± SEM in fold change, n= 3 technical repeats. Cells in (E) were compared for response to Enz (10 μM) or DMSO at the indicated study endpoints. F-G) Immunoblots and (F) cell growth analysis by colony formation assay (G) in VCaP cells lentivirally transduced with empty vector, H3.1WT, or H3.1K9M. Cells were treated for the indicated time periods with DMSO (Veh) or Enz (1μM). H) Crystal violet-stained representative images of Enz-naïve LNCaP cells expressing sgRNAs against the indicated CBX proteins or a non-targeting sgRNA, after treatment with Enz (10 μM) or DMSO (Veh) for the indicated time periods.

Figure S5

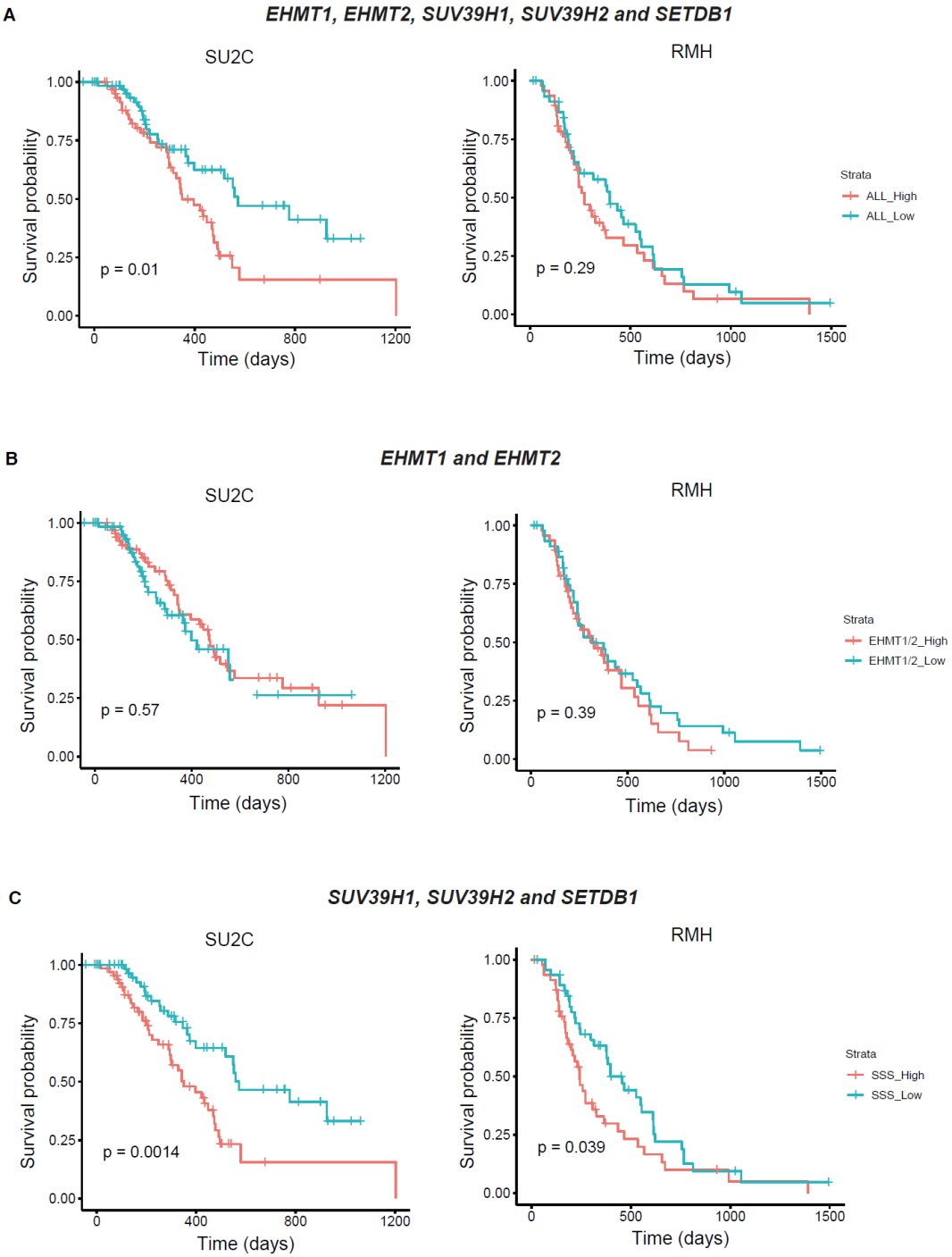

Figure S5. Elevated level of H3K9 methyltransferases is associated with poor outcomes in prostate cancer patients. A) Kaplan–Meier plots of estimated survival time based on the

combined Z-score of transcript levels of all the H3K9 methyltransferases (as indicated) in mCRPC tumor biopsies from SU2C (n=158) and Royal Marsden Hospital (RMH, n=94) cohorts. P values were calculated from a Cox proportional hazards model to determine differences in outcome between patients with high (pink) and low (green) expression. B) Same as A, except patients were stratified based on transcript levels of EHMT1/2. C) Same as A, except the patients were stratified based on transcript levels of SUV39H1, SUV39H2 and SETDB1.

Figure S6

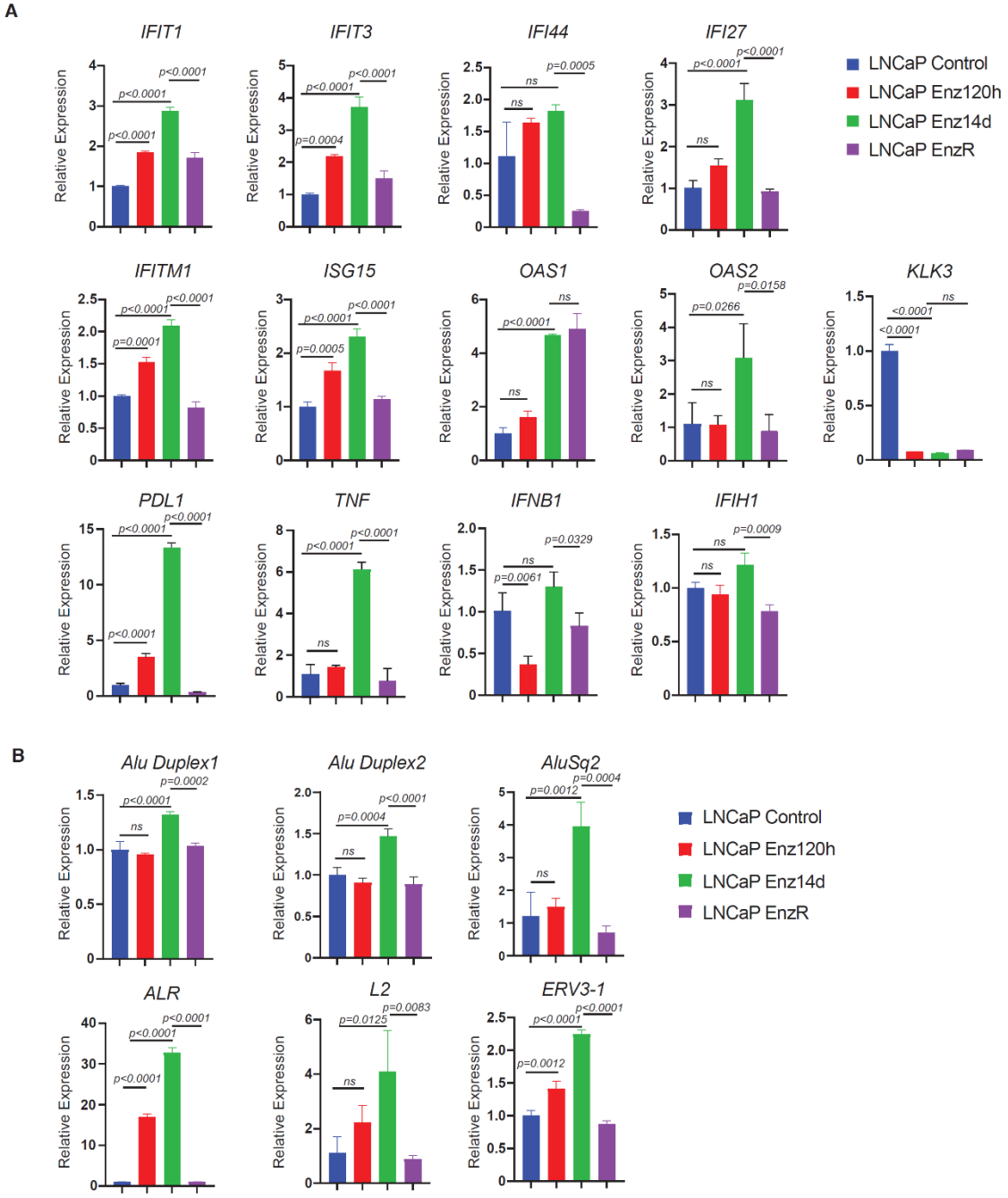

Figure S6. Enz resistance attenuates the expression of IFN-stimulated genes (ISGs) and retroelements (REs) in prostate cancer cells. A) RT-qPCR results showing the relative expression of the ISGs and *KLK3* in LNCaP cells treated with Enz (10 μM, at indicated time

points) or vehicle and LNCaP EnzR cells. B) Same as A, except RT-qPCR results showing the relative expression of the indicated retroelement transcripts. Results are representative of three biological repeats, performed in triplicates. P-value calculated using one-way ANOVA.

Figure S7

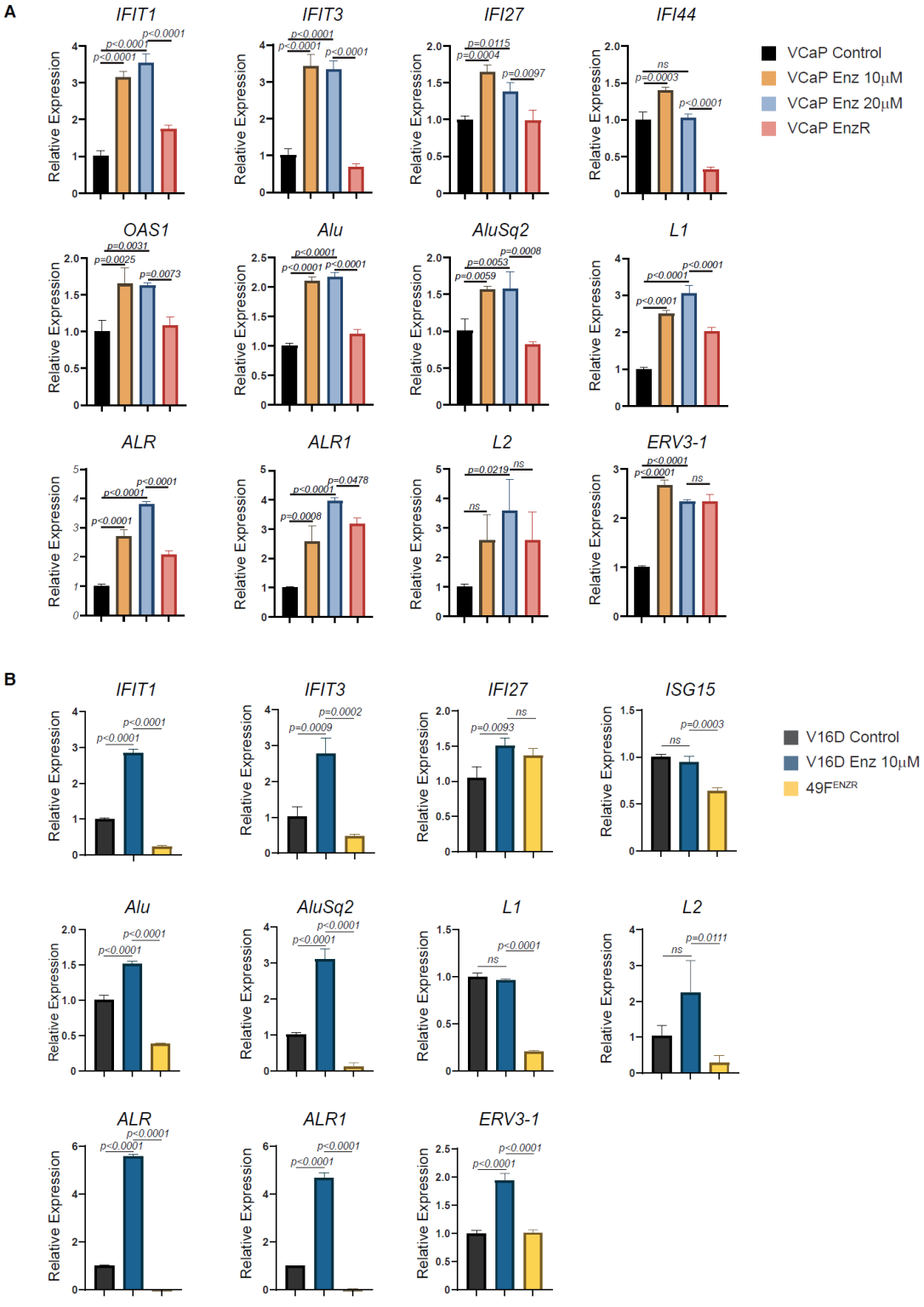
A
IFIT1
IFIT3
IFI27
IFI44
OAS1
Alu
AluSq2
L1
ALR
ALR1
L2
ERV3-1
Relative Expression
VCaP Control
VCaP Enz 10μM
VCaP Enz 20μM
VCaP EnzR
B
IFIT1
IFIT3
IFI27
ISG15
Alu
AluSq2
L1
L2
ALR
ALR1
ERV3-1
Relative Expression
V16D Control
V16D Enz 10μM
49F^ENZR

Figure S7. Enz resistance occurs with blockade of the activation of interferon signaling and retroelements in prostate cancer cells. A) RT-qPCR results showing the relative expression of the ISGs and REs in VCaP cells treated with vehicle or Enz (at indicated doses for 7 days) and VCaP EnzR cells. B) Same as A, except V16D cells were treated with vehicle or Enz (at indicated dose for 28 days) and $49F^{ENZR}$. V16D is an enzalutamide sensitive CRPC cell line developed from LNCaP cells and its derivative cell line, $49F^{ENZR}$ was developed by multiple serial transplantation of the enzalutamide-resistant tumors in athymic male mice. Results are representative of three biological repeats, performed in triplicates. P-value calculated using one-way ANOVA.

Figure S8

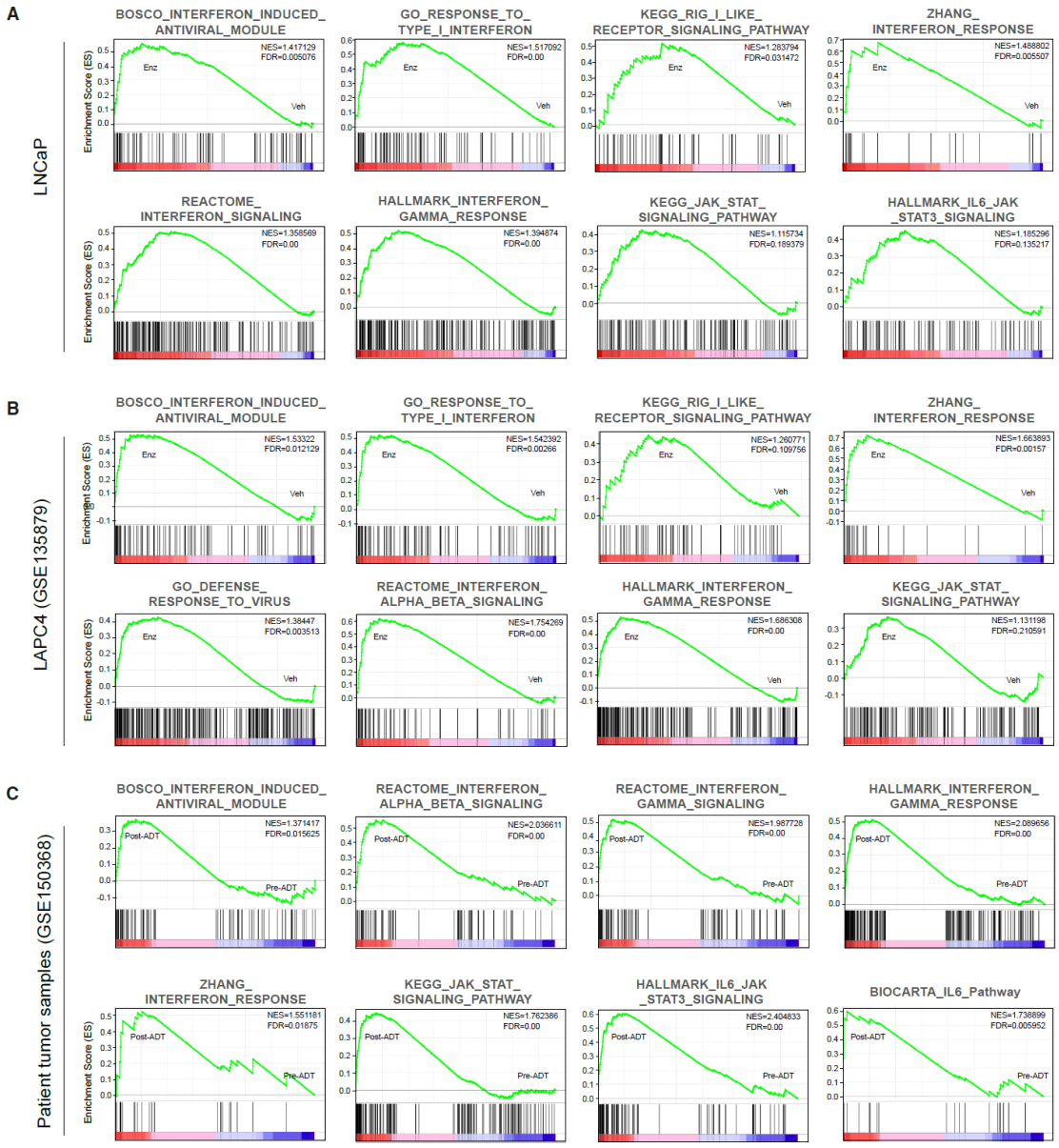

Figure S8. AR blockade and androgen-deprivation therapies induce interferon signaling pathways in prostate cancer cell lines and patient tumors. A-C) GSEA plots showing gene signatures associated with interferon pathways, IL6 signaling and viral mimicry gene signatures along with corresponding statistical metrics in (A) LNCaP cells treated with Enz (10μM) for 40 days as compared to the vehicle control, (B) LAPC4 cells treated with Enz (10μM) for 48 h as

compared to the vehicle control (GSE135879) and in (C) patient tumors subjected to androgen deprivation therapy (ADT) (GSE150368). Briefly, six paired pre- and post-ADT PCa lesions were obtained from patients with locally advanced prostate cancer who received neoadjuvant ADT (bicalutamide 50 mg per day and goserelin and 3.6 mg every 4 weeks with 2 cycles). Tissues were obtained from prostate biopsy before and after treatment.

Figure S9

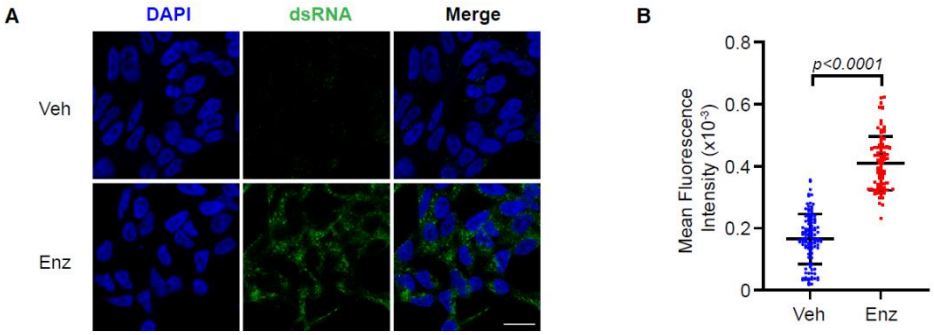

Figure S9. Enz treatment leads to formation of endogenous dsRNA.

A) Immunostaining for dsRNA in LNCaP cells treated with vehicle (DMSO) or Enz (10μM) for 72 h. Scale bar represents 20 μm. B) Dot plot representing quantification for dsRNA quantities as mean fluorescence intensity in LNCaP cells treated as indicated in panel (A).

Figure S10

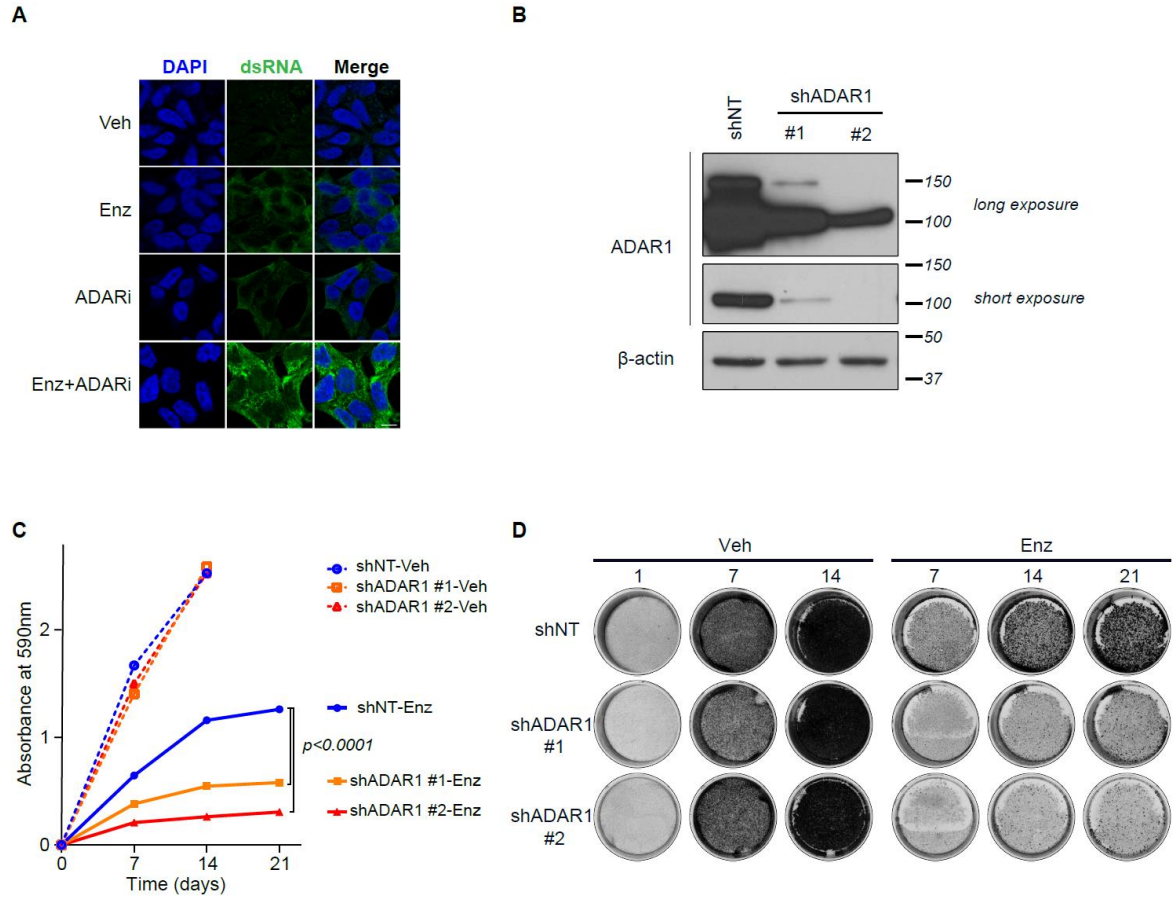

Figure S10. Loss of ADAR1 activity in combination with Enz treatment leads to accumulation of dsRNA and abrogates proliferation of prostate cancer cells. A) Immunostaining for dsRNA in LNCaP cells treated with vehicle (DMSO), Enz (10μM) and 8-Azaadenosine (ADAR1 inhibitor) alone or in combination for 72 h. Scale bar represents 20 μm. B) Immunostaining for ADAR1 using LNCaP cells that were lentivirally transduced to express shRNAs targeting ADAR1 or a non-targeting control. β-actin was used as a loading control. C-D) Cell growth analysis and representative crystal violet stained images using the same cells as in B. The cells were pretreated with Enz for 2 weeks before seeding them and treating them at the indicated time points. Treatment endpoints were compared using an unpaired *t*-test.

Figure S11

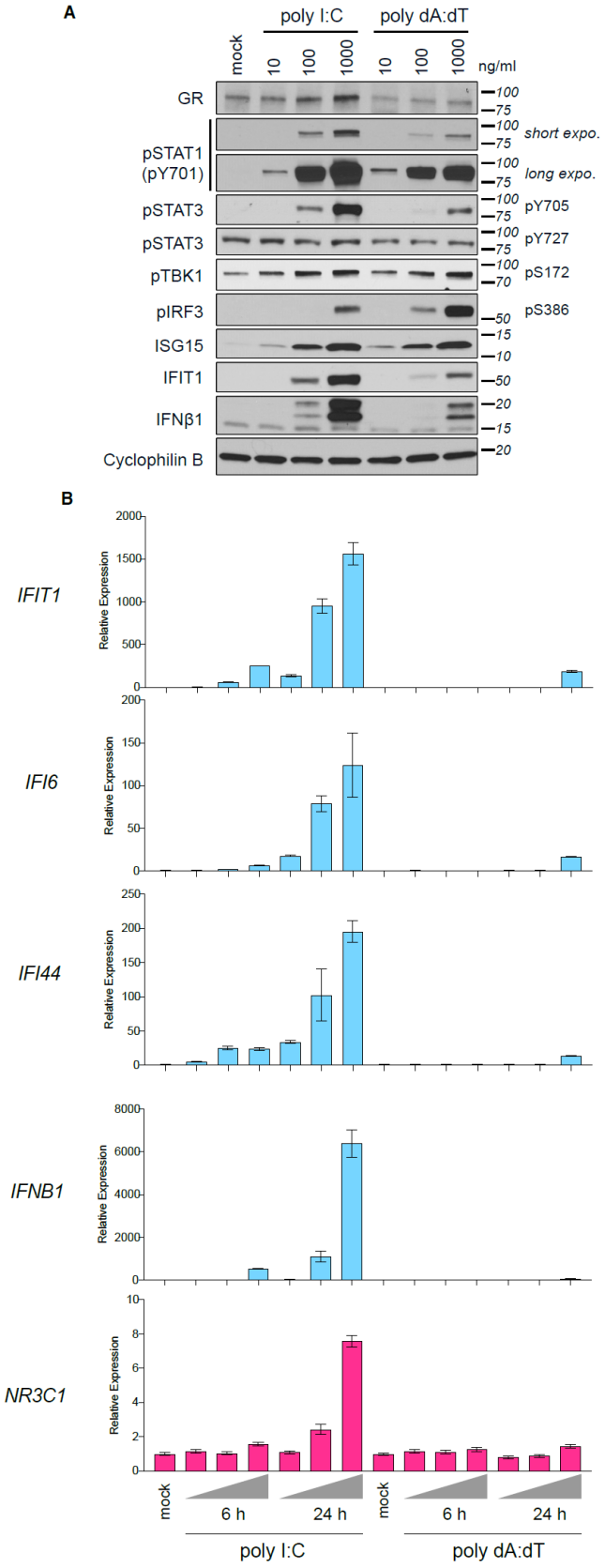
A
poly I:C
poly dA:dT
mock
10
100
1000
10
100
1000
ng/ml
GR
pSTAT1 (pY701)
short expo.
long expo.
pSTAT3
pY705
pSTAT3
pY727
pTBK1
pS172
pIRF3
pS386
ISG15
IFIT1
IFNβ1
Cyclophilin B
B
IFIT1
IFI6
IFI44
IFNB1
NR3C1
Relative Expression
mock
6 h
24 h
mock
6 h
24 h
poly I:C
poly dA:dT

Figure S11. dsRNA-induced IFN signaling triggers GR expression. A) Immunoblots of whole cell extracts from LNCaP cells, showing the expression of GR and IFN pathways regulators and products, 48 hours after transfection with poly I:C or poly dA:dT, at concentrations of 10, 100 or 1000 ng/ml. B) RT-qPCR analysis of transcript levels of NR3C1 and the indicated ISGs, 6 or 24 hours post-transfection with poly I:C or poly dA:dT as in (A). Results are representative of three biological repeats, performed in triplicates. Error bars represent SD.

Figure S12

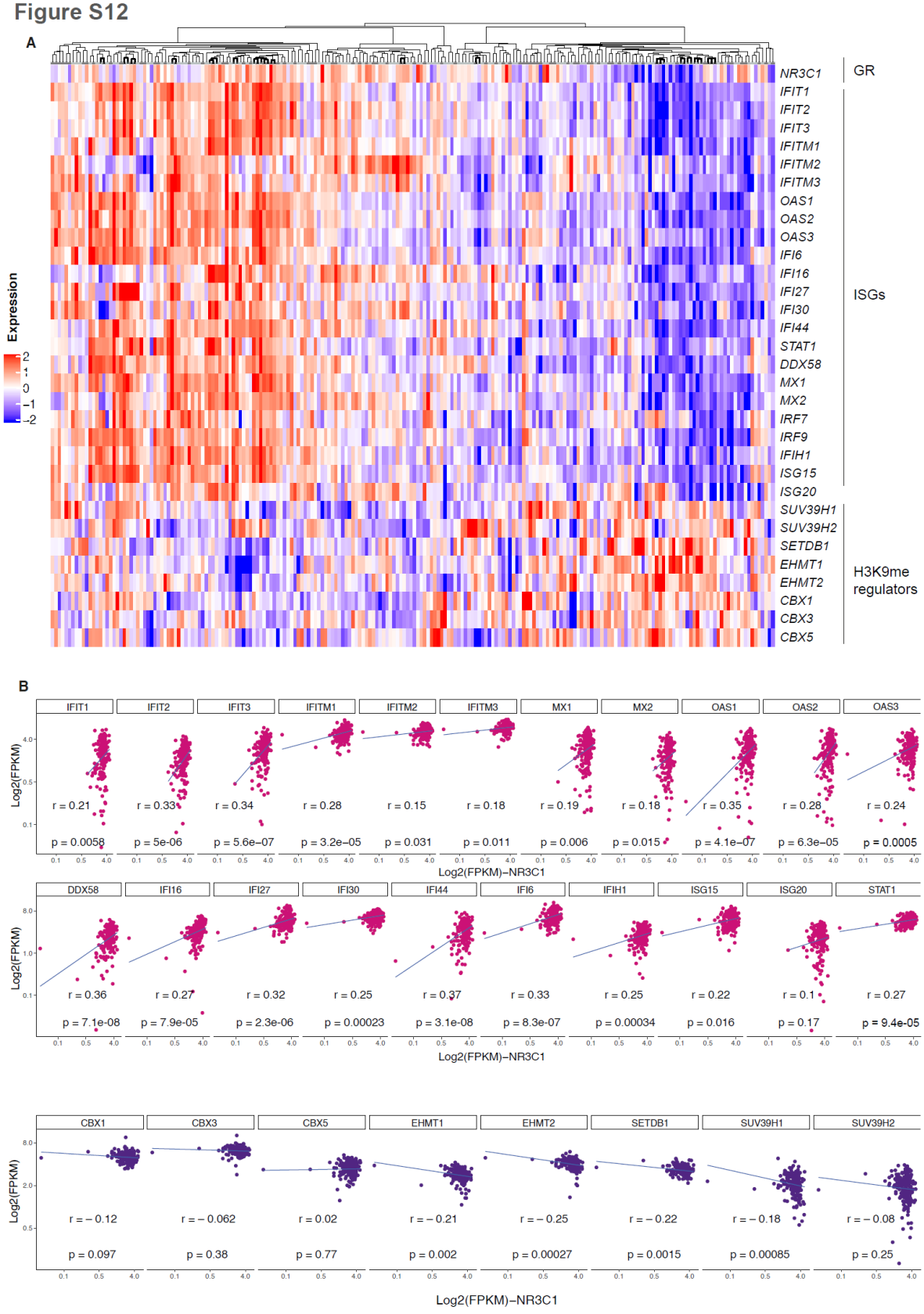
A
Expression
2
1
0
−1
−2
NR3C1
IFIT1
IFIT2
IFIT3
IFITM1
IFITM2
IFITM3
OAS1
OAS2
OAS3
IFI6
IFI16
IFI27
IFI30
IFI44
STAT1
DDX58
MX1
MX2
IRF7
IRF9
IFIH1
ISG15
ISG20
SUV39H1
SUV39H2
SETDB1
EHMT1
EHMT2
CBX1
CBX3
CBX5
GR
ISGs
H3K9me regulators
B
IFIT1 IFIT2 IFIT3 IFITM1 IFITM2 IFITM3 MX1 MX2 OAS1 OAS2 OAS3
r = 0.21 r = 0.33 r = 0.34 r = 0.28 r = 0.15 r = 0.18 r = 0.19 r = 0.18 r = 0.35 r = 0.28 r = 0.24
p = 0.0058 p = 5e-06 p = 5.6e−07 p = 3.2e−05 p = 0.031 p = 0.011 p = 0.006 p = 0.015 p = 4.1e−07 p = 6.3e−05 p = 0.0005
DDX58 IFI16 IFI27 IFI30 IFI44 IFI6 IFIH1 ISG15 ISG20 STAT1
r = 0.36 r = 0.27 r = 0.32 r = 0.25 r = 0.37 r = 0.33 r = 0.25 r = 0.22 r = 0.1 r = 0.27
p = 7.1e-08 p = 7.9e-05 p = 2.3e-06 p = 0.00023 p = 3.1e-08 p = 8.3e-07 p = 0.00034 p = 0.016 p = 0.17 p = 9.4e-05
CBX1 CBX3 CBX5 EHMT1 EHMT2 SETDB1 SUV39H1 SUV39H2
r = −0.12 r = −0.062 r = 0.02 r = −0.21 r = −0.25 r = −0.22 r = −0.18 r = −0.08
p = 0.097 p = 0.38 p = 0.77 p = 0.002 p = 0.00027 p = 0.0015 p = 0.00085 p = 0.25
Log2(FPKM)
Log2(FPKM)−NR3C1

Figure S12. Transcript levels of H3K9MTs inversely correlate with those of GR and ISGs in biopsies from patients with metastatic CRPC. A) Heatmaps representing the relative transcript levels (acquired with Capture RNA-seq platform) of GR, ISGs and H3K9MTs in biopsies from SU2C mCRPC patient cohorts (n=212). B) Pearson correlation analysis of GR mRNA levels (NR3C1) with ISGs (plots in magenta) and H3K9 methyltransferases and readers (plots in violet). r indicates the linear correlation and blue lines represent the linear fit coefficient. Significance of correlation was calculated using *t*-test.

Figure S13

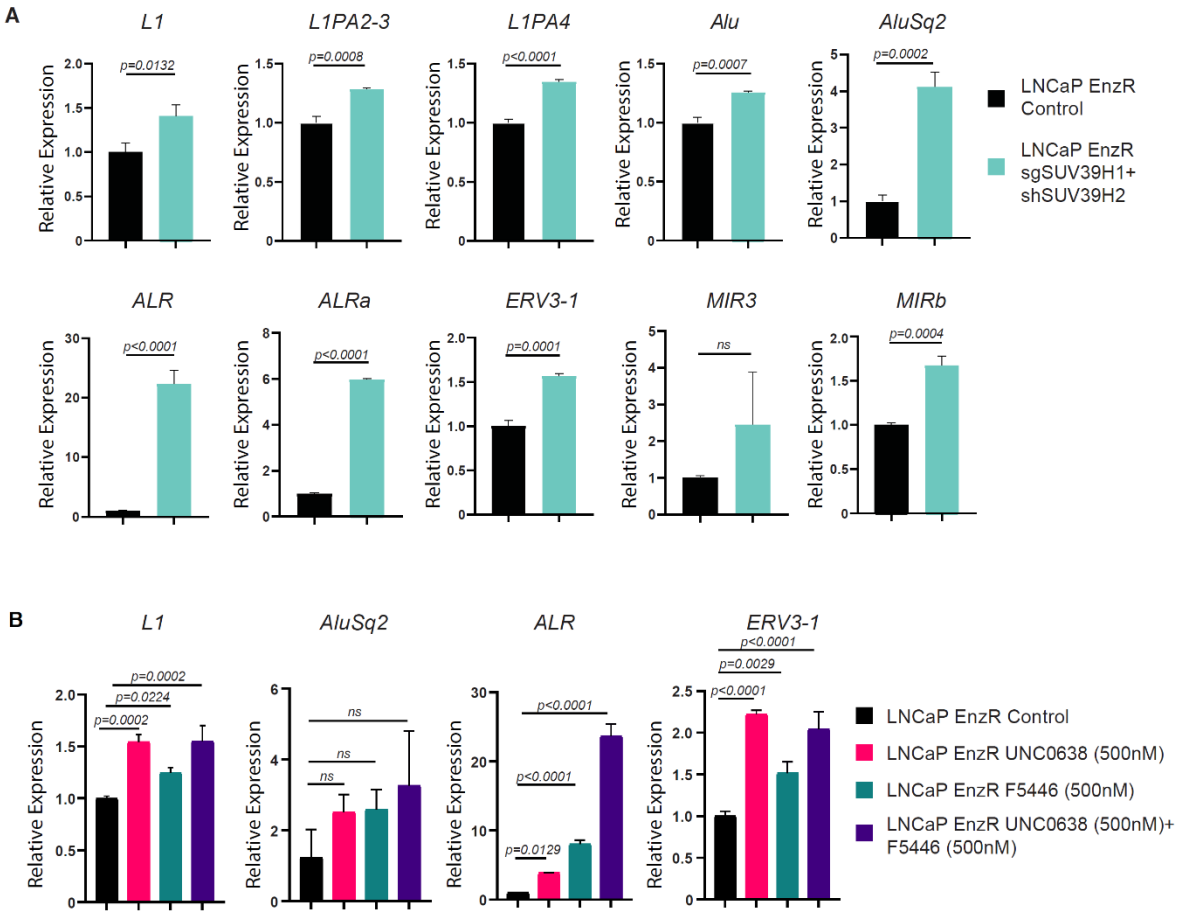

Figure S13. Genetic or pharmacological inhibition of H3K9 methyltransferases induces the expression of retroelements in Enz-resistant (EnzR) prostate cancer cells. A) RT-qPCR results showing the relative expression of the indicated retroelement transcripts in LNCaP EnzR cells with stable knockout of SUV39H1 along with knockdown of SUV39H2 as compared to non-targeting control. B) Same as A, except LNCaP EnzR cells were treated with indicated concentrations of UNC0638 (EHMT1/2 inhibitor) and F5446 (SUV39H1 inhibitor), alone or in combination as compared to vehicle control. Results are representative of three biological repeats, performed in triplicates. P-value calculated using an unpaired *t*-test in panel A and one-way ANOVA in panel B.

Figure S14

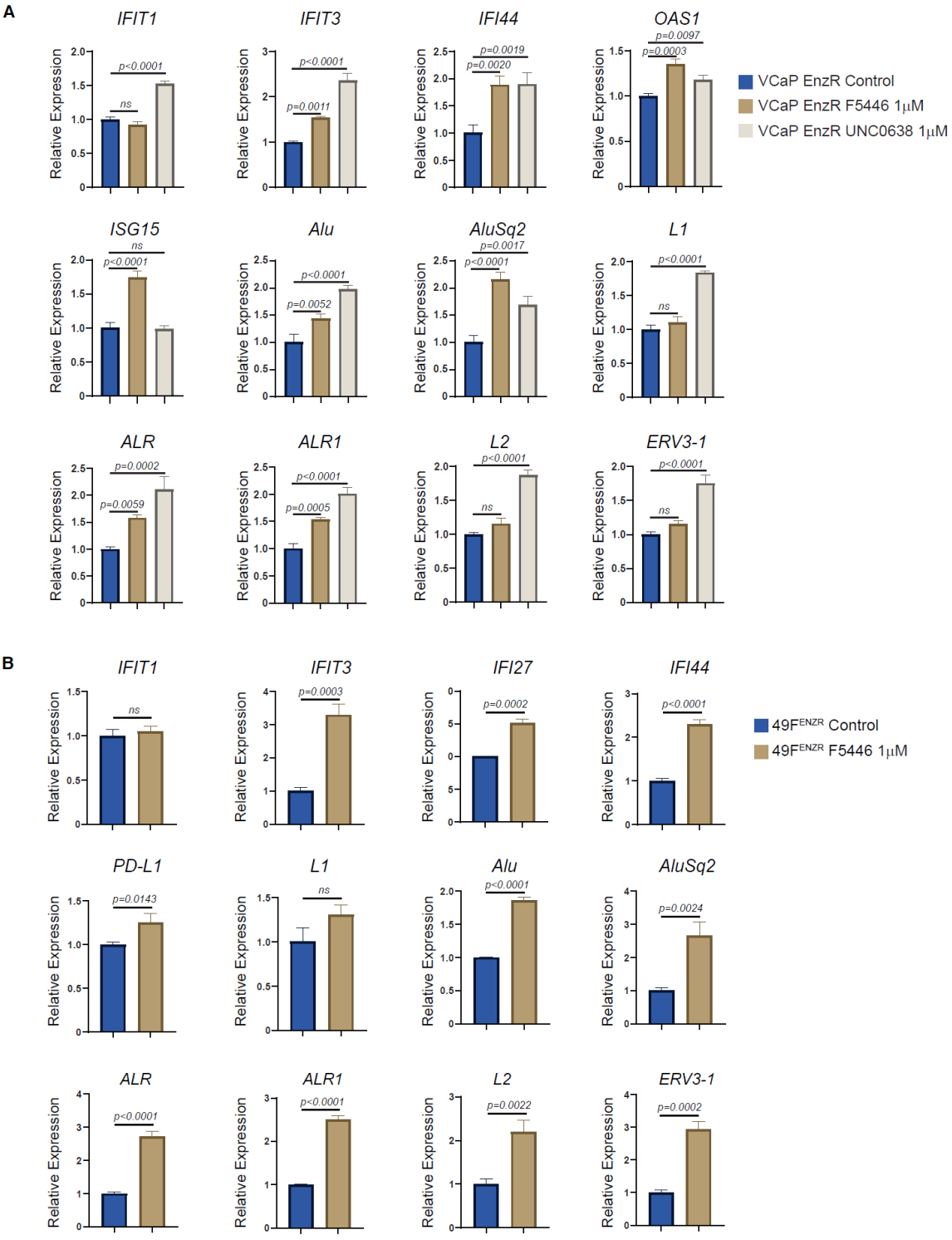
A
IFIT1
IFIT3
IFI44
OAS1
ISG15
Alu
AluSq2
L1
ALR
ALR1
L2
ERV3-1
Relative Expression
p<0.0001
ns
p=0.0011
p=0.0019
p=0.0020
p=0.0097
p=0.0003
p=0.0052
p=0.0017
p=0.0002
p=0.0059
p=0.0005
VCaP EnzR Control
VCaP EnzR F5446 1μM
VCaP EnzR UNC0638 1μM
B
IFIT1
IFIT3
IFI27
IFI44
PD-L1
L1
Alu
AluSq2
ALR
ALR1
L2
ERV3-1
p=0.0003
p=0.0002
p=0.0143
p=0.0024
p=0.0022
49F^ENZR Control
49F^ENZR F5446 1μM

Figure S14. Pharmacological targeting of SUV39H1 and EHMT1/2 induces the expression of interferon-stimulated genes and retroelements in Enz-resistant (EnzR) prostate cancer cells. A) RT-qPCR results showing the relative expression of the ISGs and REs in VCaP EnzR cells treated with indicated concentrations of F5446 (SUV39H1 inhibitor) and UNC0638 (EHMT1/2 inhibitor). B) Same as A, except $49F^{ENZR}$ cells were treated with indicated concentration of F5446 (SUV39H1 inhibitor) as compared to vehicle control. $49F^{ENZR}$ is a derivative of enzalutamide sensitive V16D cells and was developed by multiple serial transplantation of the enzalutamide-resistant tumors in athymic male mice. Results are representative of three biological repeats, performed in triplicates. P-value calculated using one-way ANOVA in panel A and an unpaired *t*-test in panel B.

Figure S15

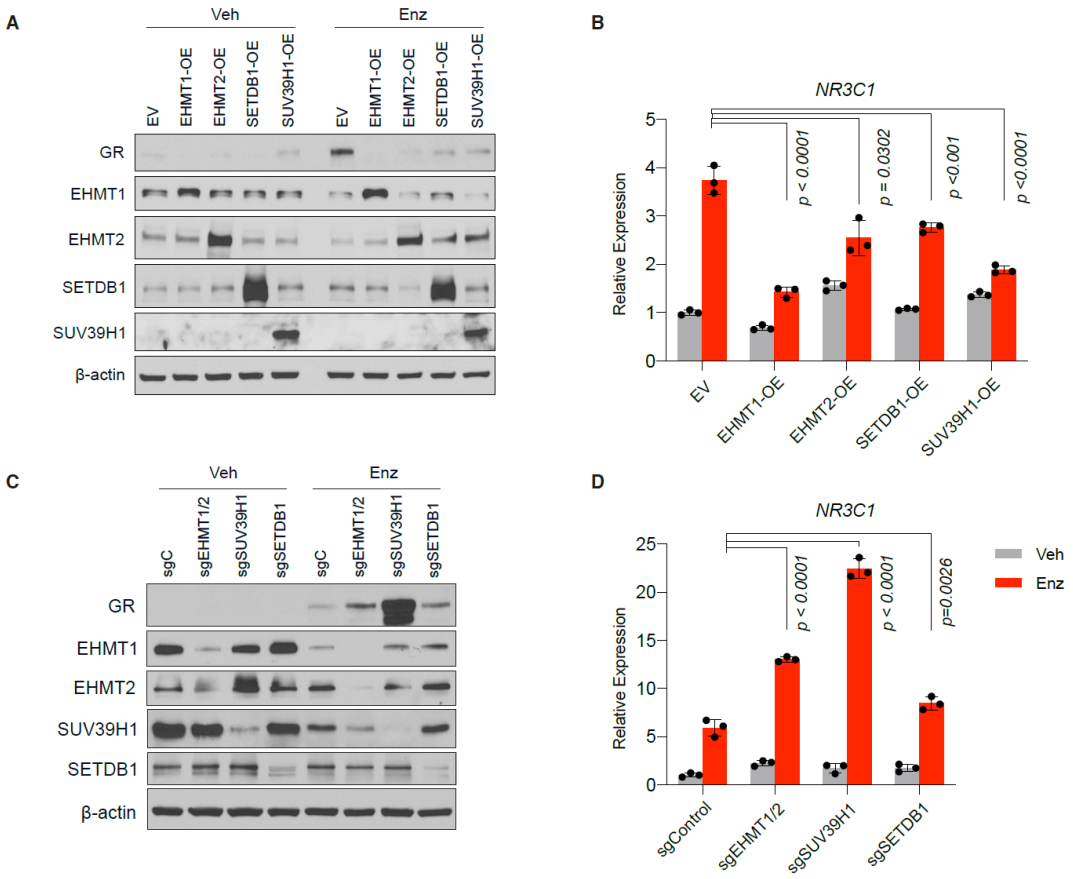

Figure S15. H3K9MTs regulate the Enz-mediated GR expression levels. A-B) Immunoblots showing overexpression efficacy (A) and RT-qPCR analysis (B) of GR levels in LNCaP cells that were lentivirally transduced to overexpress the indicated H3K9 methyltransferase after treatment with Enz (10 μM) or DMSO (Veh) for 40 days. C-D) Immunoblots (C) and RT-qPCR analysis (D) of GR expression levels in LNCaP cells that were lentivirally transduced to express guide RNAs or shRNAs targeting the indicated H3K9 methyltransferase, or a non-targeting control gRNA. Significance was calculated using two-way ANOVA; error bars represent SD. Results are representative of two biological repeats performed in triplicate.

Supplementary Methods

Lentiviral transduction, gene overexpression, knockdown, and knockout

Lentiviral particles were produced by co-transfection of 293T cells with lentivectors and the packaging plasmids psPAX2 and pMD2.G (Addgene, plasmids #12261 and #12259). The medium was changed 6 h post-transfection. Supernatants were collected 24 to 72h after transfection, passed through 0.45 µM filters and concentrated 100 times using PEG-it virus precipitation solution (System Bioscience, #LV825A-1). Cells transduced with concentrated lentivirus were selected 48 h later with the following antibiotics until all untransduced control cells were dead: 1 µg/ml puromycin (Gibco, #A1113803), 10 µg/ml blasticidin (Invivogen, #ant-bl-05), 100 µg/ml zeocin (Invitrogen, #ant-zn-05).

pDual lentivectors (a kind gift from Dr. David Escors, Fundacion Miguel Servet, Spain) which drive the expression of a transgene under the SFFV promoter and a selection marker under the ubiquitin promoter, were used for stable overexpression of H3K9MTs. pLKO.1 plasmids expressing shRNAs against SUV39H2 (TRCN0000011057 and TRCN0000006938), IFNAR1 (TRCN0000059014), ADAR1 (TRCN0000301036 and TRCN0000336886) and or the non-targeting shRNA (SHC002) were obtained from Sigma.For CRISPR-Cas9-assisted gene knockouts, guide RNAs were designed using the online CRISPR guide selection tools at crispr.mit.edu (site no longer active) or Benchling (https://benchling.com), and cloned into the lentiCRISPRv2 (Addgene, Plasmid#52961). The sgRNA oligos and target sequences for each gene are listed in **Table S1**. LentiCRISPRv2-MAVS was a kind gift from Dr. Susan Weiss (University of Pennsylvania, Philadelphia, USA).

Cell growth and proliferation assays

For growth monitoring by crystal violet assay, 1 to $2x10^5$ cells were seeded in 6-well plates 24 h prior to initiation of treatment. Cells were replenished with fresh media containing DMSO or Enz (5-10 μM) every 3 days, without disturbing the attached monolayer. Cells in the Enz group were usually pre-treated with Enz for 14 to 90 days before seeding, as specified in the pertinent figure legends. At treatment endpoints, medium was gently aspirated from the wells, then 2 mL fixing/staining solution (0.1% crystal violet, 1% formaldehyde [37%], 1% methanol in PBS) was added to each well, followed by incubation at room temperature for 15 min. Plates were washed by dipping into a bucket of water filled with a gentle stream of tap water, air-dried and then imaged with the ChemiDoc imaging system (Bio-Rad). Differences in cell growth between experimental groups were quantified using a colorimetric assay. Crystal violet dye in each well was eluted by adding 4 mL 10% acetic acid and incubating for 30 min at room temperature with gentle agitation. The dissolved dye was further diluted 1:4 and optical density was measured at 590 nm using a SpectraMax i3x microplate reader (Molecular Devices).

Cell proliferation was monitored using the IncucyteZoom live-cell analysis system (Essen Bioscience). Briefly, 10^4 cells were seeded in 12-well plates and imaged every 3 h. Media supplemented with treatment compounds were refreshed every 3 days. The percentage of cell confluence was estimated from an average of 9 images/well at each time point and presented as mean ± SEM.

Immunoblotting

Whole cell extracts were prepared using RIPA lysis buffer (Sigma, R0278) containing Halt phosphatase and protease inhibitor cocktail (Thermo Fisher, 78440) and 20 cycles of sonication with the Diagenode Bioruptor on the high setting (30 s on/30 s off). Cytoplasmic, nuclear, and

chromatin-bound fractions then were extracted using a subcellular fractionation kit (Pierce, 78840). The chromatin-bound pellets were washed twice with ice-cold PBS, before sonicating for 20 cycles at the high setting. Core histones were isolated using a histone purification kit (Active Motif, #40026) following the manufacturer's instructions. Lysate protein quantities were then measured using the Pierce BCA Protein Assay Kit (#23225). Lysates were mixed with 4X Laemmli buffer and heated at 95ºC for 5 min to denature. Samples were separated on 8% to 12% SDS-polyacrylamide gels and wet-transferred to 0.45μM PVDF membranes (Millipore, #IPVH00010) which were then blocked with 5% skimmed milk in TBS-T (0.1% Tween 20 in 50 mM Tris-HCl, pH 7.6, and 150 mM NaCl) for 1 h at room temperature. Membranes were incubated with desired concentrations of primary antibodies in blocking buffer overnight at 4ºC. After TBS-T washes, membranes were incubated with HRP-conjugated anti-rabbit IgG (Thermo Scientific, TK274616) or anti-mouse IgG (GE Healthcare, NXA931) secondary antibodies diluted in blocking buffer for 1 h at room temperature. Bound antibodies were visualized by the ECL systems (LumiGLO, #5430-0040 or LumiGLO Reserve, #5430-0051, Seracare).

The primary antibodies consisted of: SETDB1 (Proteintech, 11231-1-AP), SUV39H1 (Cell Signaling, #8729), SUV39H2 (Abcam, #ab190870), EHMT1 (Bethyl Laboratories, #A301-642A), EHMT2 (Proteintech, #66689-1-Ig; Cell Signaling, #3306), KDM3A (Proteintech, #12835-1-AP), KDM4A (Bethyl Laboratories, #A300-861A), KDM4B (Bethyl Laboratoris, #A301-478A), CBX1 (Cell Signaling, #8676), CBX3 (Cell Signaling, #2619), CBX5 (Cell Signaling, #2616), MeCP2 (Cell Signaling, #3456), GR (BD Biosciences, #611227), pSTAT1 pY701(Cell Signaling, #9167), pSTAT3 pY705(Cell Signaling, #9145), pSTAT3 pS727(Cell Signaling, #9134), pTBK1 pS172 (Cell Signaling, #5483; Abcam, #ab109272), pIRF3(Cell Signaling, #37829), MAVS(Cell Signaling, #24930), ISG15 (Proteintech, #15981-1-AP), IFIT1 (Proteintech, #23247-1-AP),

IFNB1 (Cell Signaling, #73671, PSA (Cell Signaling, #5361), ADAR1 (Cell Signaling #8124) ACTB (Cell Signaling, #2409), GAPDH (Cell Signaling, #2118), cyclophilin B (Cell Signaling, #43603), histone H3 (Abcam, #ab1791; Cell Signaling, #4499), H3K9me1(Abcam, #ab8896), H3K9me2(Cell Signaling, #4658), H3K9me3 (Abcam, #8898; Active Motif, #39062), H3K9ac (Cell Signaling, #9649), H3K9M (Cell Signaling, #78087).

Quantitative RT-PCR

Total RNA was extracted from cells using TRIzol reagent (Invitrogen, #15596018) or RNeasy Mini Kit (Qiagen, # 74106) following manufacturer's protocol. cDNA was made from 1µg RNA using iScript cDNA Synthesis Kit (Bio-Rad, # 1708890). Quantitative PCR (qPCR) analysis was performed in an ABI 7500 Real-Time PCR machine (Applied Biosystems) using iTaq Fast SYBR Green Supermix with ROX (Bio-Rad, # 172-5101). Primers were designed with Primer3 online tool (https://bioinfo.ut.ee/primer3-0.4.0/) and synthesized with Integrated DNA Technologies, Inc. (IDT). Relative quantities of each transcript were determined by first normalizing to *RPLP0* levels and then, vehicle treated control cells. All shown gene expression studies are a representative of three biological repeats, performed in technical triplicates using the primers listed in **Table S2**.

RNA-seq data analysis

Libraries were prepared using Roche Kapa mRNA HyperPrep strand specific sample preparation kits from 200ng of purified total RNA according to the manufacturer's protocol on a Beckman Coulter Biomek i7. The finished dsDNA libraries were quantified by Qubit fluorometer, Agilent TapeStation 2200, and RT-qPCR using the Kapa Biosystems library quantification kit according to manufacturers' protocols. Uniquely dual indexed libraries were pooled in equimolar ratios and sequenced on an Illumina NovaSeq 6000 with paired-end 50bp reads by the Dana-Farber Cancer Institute Molecular Biology Core Facilities. Reads were aligned to the UCSC hg19 reference

genome, and gene counts were quantified using STAR (v2.5.1b) (1). Normalized gene expression in fragments per kilobase million (FPKM) was calculated using cufflinks (v2.2.1) (2) and in transcripts per kilobase million (TPM) using adapted code (3, 4). RNA-seq analysis was performed using the VIPER pipeline (5).

Gene set enrichment analysis (GSEA)

For GSEA, gene expression data were derived from either our own study or publicly available datasets (GSE135879 and GSE150368, GSE99381). The expression data between two different phenotypes were compared using the gene sets obtained from the Molecular Signatures Database (MSigDB, v7.2) (6).

ChIP-seq data generation and analysis

ChIP-seq analysis was performed on Enz-naïve LNCaP cells treated either with vehicle or Enz 10 μM for 120 h, and on Enz-resistant cells maintained in media containing Enz 10 μM. Briefly, cells were fixed with 1% formaldehyde for 15 min followed by quenching with 0.125 M glycine. Chromatin was obtained by adding lysis buffer (50 mM Tris-HCl pH 8, 1% SDS, 10 mM EDTA), followed by disruption with a Dounce homogenizer. The cell lysates were sonicated using Bioruptor from Diagenode, shearing the DNA to an average length of 300-500 bp. The input DNA was prepared by treating aliquots of chromatin with proteinase K and RNase along with heat for de-crosslinking followed by ethanol precipitation. The resulting DNA was resuspended and quantified on a NanoDrop spectrophotometer. For each condition, ~40 μg of chromatin was precleared using protein A agarose beads (Invitrogen) and immunoprecipitation was performed using 4 μg antibody against H3K9me2 (Active Motif, #39239) and H3K9me3 (Active Motif, #39161). The immuno-complexes were then washed and eluted from the beads followed by subjecting them RNase A and Proteinase K treatment. The reverse crosslinking was performed by

incubating the samples at 65ºC overnight, and ChIP DNA was purified by phenol-chloroform extraction and ethanol precipitation. qPCR reactions were carried out in triplicate on specific genomic regions using SYBR Green Supermix (Bio-Rad). The resulting signals were normalized for primer efficiency by carrying out qPCR for each primer pair using input DNA.

Illumina sequencing libraries were prepared from input and ChIP DNAs by the standard consecutive enzymatic steps of end-polishing, dA-addition, and adaptor ligation. Steps were performed on an automated system (Apollo 342, Wafergen Biosystems/Takara). After a final PCR amplification step, the resulting DNA libraries were quantified and sequenced on Illumina's NextSeq 500 (75 nt reads, single end). Reads were aligned consecutively to the human genome (hg38) (7). Duplicate reads were removed, and only uniquely mapped reads (mapping quality ≥ 25) were used for further analysis. Human alignments were extended in silico at their 3′-ends to a length of 200 bp, which is the average genomic fragment length in the size-selected library and assigned to 32-nt bins along the genome. The resulting histograms (genomic "signal maps") were stored in BigWig files. Peak locations were identified using the SICER algorithm (8) at a cutoff of FDR 1E-10 and a max gap parameter of 600 bp. Peaks that were on the ENCODE blacklist of known false ChIP-Seq peaks were removed. Signal maps and peak locations were used as input data in Active Motif's proprietary analysis program, which creates Excel tables containing detailed information on sample comparison, peak metrics, peak locations, and gene annotations.

Repeat element annotations of ChIP-seq data

The catalogues of peaks generated as described above were further filtered to produce stringent signatures of peaks associated with different treatment conditions by applying a minimum fold change threshold of 1.5 in the read count signal compared to each of the other two groups. Peak filtration was performed separately for H3K9me2 and H3K9me3 datasets. These were then

annotated based on associations with genomic features using the R package ChipSeeker (9), paired with annotations from the TxDb.Hsapiens.UCSC.hg38.knownGene Bioconductor package.

The RepeatMasker UCSC genome track was used to locate repeats in the genome, and peaks were then mapped to overlapping repeats using these annotations (10). Class and family annotations were then used to calculate both the raw overlaps and normalized overlaps (percent of peaks mapping to a repeat class/family) to examine whether certain categories of repeats were overrepresented using the genomation R package. Heatmaps of genomic features were visualized using the genomation R package. Once filtered peak sets were derived, data were normalized to rpm and 10 kb regions, with the peak midpoint at the center, and the genomic intervals were visualized using the genomation R package. RPM values were binned into 400 windows of 25bp each.

dsRNA Immunofluorescence

Cells were grown on glass coverslips and fixed with 4% paraformaldehyde. The cells were washed thrice with PBS, followed by permeabilization with 0.3% Triton X-100 in PBS (PBS-T) for 10 min at room temperature. Cells were then blocked with 5% normal goat serum in PBS-T for 2 h at room temperature and incubated with primary antibody (SCICONS anti-dsRNA mAb J2, Cat# 10010200, 1:400) overnight at 4°C. The cells then were washed 3 times in PBS and incubated with fluorophore-conjugated anti-mouse secondary antibody (CST anti-mouse IgG Alexa Fluor® 488 Conjugate, Cat#4408, 1:1200) for 1h to 2 h at room temperature. The cells were again washed 3 times with PBS and counterstained with DAPI. The coverslips were mounted on glass slides using Vectashield (Vector Laboratories). The ADAR1 inhibitor, 8-Azaadenosine used in the immunofluorescence experiments was procured from MedChemExpress (Cat. No.: HY-115686). Images were acquired using a Leica TCS-SP8-AOBS inverted confocal microscope (Leica

Microsystems, GmbH, Wetzlar, Germany). For quantification, the images were acquired at 63X magnification and mean fluorescence intensity (MFI) for dsRNA was determined using the pipeline derived from the CellProfiler image analysis software (11).

Histone mass spectrophotometry procedures and data analysis

Bulk histones were acid-extracted from frozen cell pellets, propionylated, and trypsin-digested as described previously (12). Briefly, histones were extracted by incubating samples at room temperature for 1 h in 0.2M sulfuric acid with intermittent vortexing. Histones were then precipitated by the addition of trichloroacetic acid (TCA) on ice, and recovered by centrifugation at 10,000 × *g* for 5 min at 4°C. The pellet was then washed once with 1 mL cold acetone/0.1% HCl and twice with 100% acetone, and then air-dried in a clean hood. The histones were propionylated by adding 1:3 v/v propionic anhydride/2-propanol and incrementally adding ammonium hydroxide to keep the pH near 8, and subsequently dried in a SpeedVac concentrator. The pellet was then resuspended in 100 mM ammonium bicarbonate and adjusted to pH 7-8 with ammonium hydroxide. The histones were then digested with trypsin resuspended in 100 mM ammonium bicarbonate overnight at 37°C and dried in a SpeedVac concentrator. The pellet was resuspended in 100 mM ammonium bicarbonate and propionylated a second time by adding 1:3 v/v propionic anhydride/2-propanol and incrementally adding ammonium hydroxide to keep the pH near 8, and subsequently dried in a SpeedVac concentrator. Histone peptides were resuspended in 0.1% TFA in H_2O for mass spectrometry analysis.

Mass spectrometry samples were analyzed on a triple quadrupole (QqQ) mass spectrometer (Thermo Fisher Scientific TSQ Quantiva) directly coupled with an UltiMate 3000 Dionex nano-liquid chromatography system. Peptides were first loaded onto an in-house packed trapping column (3cm×150μm) and then separated on a New Objectives PicoChip analytical column (10

cm×75 μm). Both columns were packed with New Objectives ProntoSIL C18-AQ, 3μm, 200Å resin. The chromatography gradient was achieved by increasing percentage of buffer B from 0 to 35% at a flow rate of 0.30 μl/min over 45 min. Solvent A was 0.1% formic acid in water, and B was 0.1% formic acid in 95% acetonitrile. The QqQ settings were as follows: collision gas pressure of 1.5 mTorr; Q1 peak width of 0.7 (FWHM); cycle time of 2 s; skimmer offset of 10 V; electrospray voltage of 2.5 kV. Targeted analysis of unmodified and various modified histone peptides was performed. This entire process was repeated 3 separate times for each sample.

Raw MS files were imported and analyzed in Skyline with Savitzky-Golay smoothing (13). All Skyline peak area assignments for monitored peptide transitions were manually confirmed. A minimum of 3 peptide transitions were quantified for each modification. For each monitored amino acid residue, each modified (and unmodified) form was quantified by first calculating the sum of peak areas of corresponding peptide transitions; the sum of all modified forms was then calculated for each amino acid to represent the total pool of modifications for that residue. Finally, each modification was then represented as a percentage of the total pool of modifications. This process was carried out for each of the three separate mass spec runs, and the raw data provided in the data delivery spreadsheet corresponds to the mean and standard deviation of the resulting three values from this analysis for each modified and unmodified form of the corresponding amino acid residue.

To generate the heatmaps found in the data delivery spreadsheet, for each individual modification and each unmodified form, the data for each sample was converted to the fraction of the sum across all samples to display relative abundances across the sample group, and then conditionally formatted in Excel using the default red/white/blue color scheme. The hierarchical clustering heatmap was generated in R using the “pheatmap” function with default settings. The PCA plot was also generated in R using the first two principal components to generate an XY plot.

Supplementary Tables

Table S1. Sequences of gRNA oligos cloned into lentiCRISPRv2

Target gene	name		Sequence (5'→3')
EHMT1	sgEHMT1-2	forward	CACCG***CGCTATCCGAGTTAGTGTGT***
		reverse	AAAC***ACACACTAACTCGGATAGCG***C
	sgEHMT1-3	forward	CACCG***TAACTCGGATAGCGGAAAAT***
		reverse	AAAC***ATTTTCCGCTATCCGAGTTA***C
EHMT2	sgEHMT2-2	forward	CACCG***GGAAGAGAGAGTAGGCTCCG***
		reverse	AAAC***CGGAGCCTACTCTCTCTTCC***C
	sgEHMT2-3	forward	CACCG***CTGCTGGAGAAGGAAACCAG***
		reverse	AAAC***CTGGTTTCCTTCTCCAGCAG***C
SETDB1	sgSETDB1-6	forward	CACCG***GCATCCAAACCAATGCACCC***
		reverse	AAAC***GGGTGCATTGGTTTGGATGC***C
	sgSETDB1-9	forward	CACCG***TTAAGGCAGCCATAGCTTCA***
		reverse	AAAC***TGAAGCTATGGCTGCCTTAA***C
SUV39H1	sgSUV39H1-9	forward	CACCG***CTGCCCTCGGTATCTCTAAG***
		reverse	AAAC***CTTAGAGATACCGAGGGCAG***C
	sgSUV39H1-10	forward	CACCG***GGATCTTCTTGTAATCGCAC***
		reverse	AAAC***GTGCGATTACAAGAAGATCC***C
CBX1	sgCBX1-1	forward	CACCG***CTCGACCGTCGAGTGGTAAA***
		reverse	AAAC***TTTACCACTCGACGGTCGAG***C
	sgCBX2-2	forward	CACCG***AAAAGTTCTCGACCGTCGAG***
		reverse	AAAC***CTCGACGGTCGAGAACTTTT***C
CBX3	sgCBX3-1	forward	CACCG***AGACTTGGTGCTGGCGAAAG***
		reverse	AAAC***CTTTCGCCAGCACCAAGTCT***C
	sgCBX3-3	forward	CACCG***AGAGCCTGAAGAATTTGTCG***
		reverse	AAAC***CGACAAATTCTTCAGGCTCT***C
CBX5	sgCBX5-3	forward	CACCG***CAGAGCAATGATATCGCTCG***
		reverse	AAAC***CGAGCGATATCATTGCTCTG***C
	sgCBX5-4	forward	CACCG***GACATGGCATGCATATCCTG***
		reverse	AAAC***CAGGATATGCATGCCATGTC***C
MAVS	sgMAVS-1	forward	CACCG***GAGGGCTGCCAGGTCAGAG***
		reverse	AAAC***CCTCTGACCTGGCAGCCCT***C
Non-targeting control	sgControl	forward	CACCG***ATCTGCCATGGCGTCCTGGC***
		reverse	AAAC***GCCAGGACGCCATGGCAGAT***C

Nucleotides sequences in bold and italic indicate the gRNA target sequences.

Table S2. Primers used for qPCR analysis

Gene name		**Sequence (5'→3')**
EHMT1	forward	TCAAGGTCCACAGGGCACG

	reverse	TAGCGACTGATGAAGGGATGGGAA
EHMT2	forward	TTAGACAACAAGGATGGAGAGGTG
	reverse	CGGGAACTGAAGAAGGCGATG
SETDB1	forward	CTGGAGAACTAAGCAAAGATGGTGA
	reverse	CAGGAGGGTGGTAATCATAGGCAA
SUV39H1	forward	GCTATGACTGCCCAAATCGTGT
	reverse	AATCTTCTCCAGGGTGCGGA
SUV39H2	forward	AGGCACACAGTATTCGCTTTG
	reverse	CGTGATTCCCTTGTTGTCATAGA
CBX1	forward	CTGAAGATAAGGGAGAGGAGAGCA
	reverse	TGGGCACTTGACATTGGCTT
CBX3	forward	AGTGGAAGGGATTTACAGATGC
	reverse	CTCTTGGTTTGTCAGCAGCA
CBX5	forward	AAACTTGGATTGCCCTGAGC
	reverse	GTTACTTTCTGACTTCTCCCTGG
KLK3	forward	GCAGCATTGAACCAGAGGAGTT
	reverse	AGCGTCCAGCACACAGCAT
NR3C1	forward	GTTTCTGCGTCTTCACCCTCAC
	reverse	CCCAGGTCATTTCCCATCACTTT
IFIT1	forward	CCTTGCTGAAGTGTGGAGGA
	reverse	CCAGGCGATAGGCAGAGAT
IFIT2	forward	ATTCACCTCTGGACTGGCAATA
	reverse	CACCTTCCTCTTCACCTTCTTCAC
IFIT3	forward	AACTACGCCTGGGTCTACTATCAC
	reverse	CTTCGCCCTTTCATTTCTTCCACA
IFITM1	forward	GCCAAGTGCCTGAACATCT
	reverse	CACAGAGCCGAATACCAGTAAC
IFI6	forward	TGAGCTGGTCTGCGATCCTG
	reverse	CGAGATACTTGTGGGTGGCG
IFI27	forward	ATCGCCTCGTCCTCCATAGC
	reverse	GAGAGTCCAGTTGCTCCCAGT
IFI44	forward	TGTGAGCCTGTGAGGTCCAA
	reverse	GCAGCCCATAGCATTCGTCTC
ISG15	forward	GTGGTGGACAAATGCGACGAAC
	reverse	CTTGCTGCTTCAGGTGGGC
OAS1	forward	CGATGTGCTGCCTGCCTT
	reverse	AAGTCTCTCTGTAGTTCTGTGAAGC
OAS2	forward	GAATACCTGAAGCCCTAC
	reverse	CTGAAGAAGAGGACAAGG
OAS3	forward	ACTCCTGACTGTGTATGCCTG
	reverse	GTCTTGTCCTTGGCGTTGTAGTT
OASL	forward	ACTCCTTCGTGGCTCAGTGG
	reverse	CACCTTGACTACCTTCAGCACC
IFIH1	forward	TTCCGCTATCTCATCTCGTGCTT
	reverse	ACTGTCCTCTGAATCTGCTCCTTC

IFNB1	forward	GGACGCCGCATTGACCATC
	reverse	AGACATTAGCCAGGAGGTTCTCA
IL6	forward	CTTCGGTCCAGTTGCCTTCTCC
	reverse	GGTGAGTGGCTGTCTGTGTGG
TNF	forward	CAACCTCCTCTCTGCCATCAAGA
	reverse	ATCCCAAAGTAGACCTGCCCA
PDL1	forward	CACACTGAGAATCAACACAACAAC
	reverse	TGCTACACCAAGGCATAATAAGAT
IFNAR1	forward	TTTAGTGACGCTGTATGTG
	reverse	TAAGTGATGGAAAGAAGACA
Alu	forward	CAACATAGTGAAACCCCGTCTC
	reverse	GCCTCAGCCTCCCGAGTAG
AluSq2	forward	AAGTGTCACCTCCCCATCTG
	reverse	ACCACCGTTTCCTGAGCTT
AluSx	forward	AATTCAACTATATTAAAACACTTCAGA
	reverse	GACTTGAAGCTTTGACAGCA
MIR3	forward	GTGGAAAGAACAACTGGACTAGG
	reverse	GCCCAGAGAGGTGAAGTGA
MIRb	forward	CTTACTAGCTGTGTGACCTTGG
	reverse	ACCCTGCGAGGTAGGTATTA
MIRc	forward	GGGCAAGTCACTTAACCTCTC
	reverse	ATCCTCACAACAACCCTGTG
L1Hs_ORF1	forward	GGTTACCCTCAAAGGAAAGCC
	reverse	GCCTGGTGGTGACAAAATCTC
L1Hs_ORF2	forward	AAATGGTGCTGGGAAAACTG
	reverse	GCCATTGCTTTTGGTGTTTT
L1PA2-3	forward	GGAAATCATCATTCTCAGTAAAC
	reverse	CACAGTCCCCAGAGTGTGATAT
L1PA4	forward	TCACCAATATCCGCTGTTCTG
	reverse	GTCTGTTGGAGTTTACTGGAGG
L1PA10	forward	TGGAACCAAGTTGGAAAACA
	reverse	TTGGCCTGTCTTGCTAGGTT
L2	forward	TCTACACTCACTCCCTTGGT
	reverse	AGGTCTGGGCTGGAGATATAA
L2D	forward	CTTCCTCCCTTTCTTCTCCAAA
	reverse	ATCAATGTGGGCTGGAGTG
ALR	forward	CGATCCTTTACACAGAGCAGAC
	reverse	ACCTCAAAGCGGCTGAAAT
ALR1	forward	GAGCAGTTTGGAAACACTCTG
	reverse	GAAATCCCGTTTCCAACGAAG
ALRa	forward	CTGAGAAACTGCTTTGTGATGTG
	reverse	CAGTGTTTCCAAACTGCTGAAT
ALRb	forward	GCAAGTGGAGATTTCAAGCG
	reverse	GCTCTGTCTAAAGGAAGGTTCA
ERV3-1	forward	AGGAAGAGGGAGTATGCGGAAAG

	reverse	CAAGTCTGAACTGGGATGTGAGC
ERVW-1	forward	GCAATACTACATACACAACCAACTCC
	reverse	GGCACTAAGAATGAGAGGAAGCAC
MER21C	forward	GGAGCTTCCTGATTGGCAGA
	reverse	ATGTAGGGTGGCAAGCACTG
MLT1C49	forward	TATTGCCGTACTGTGGGCTG
	reverse	TGGAACAGAGCCCTTCCTTG
RPLP0	forward	ATTACACCTTCCCACTTGCTG
	reverse	ACTCTTCCTTGGCTTCAACCTTA

Supplementary References

1. A. Dobin, *et al.*, STAR: Ultrafast universal RNA-seq aligner. *Bioinformatics* (2013) https:/doi.org/10.1093/bioinformatics/bts635.
2. C. Trapnell, *et al.*, Transcript assembly and quantification by RNA-Seq reveals unannotated transcripts and isoform switching during cell differentiation. *Nat. Biotechnol.* (2010) https:/doi.org/10.1038/nbt.1621.
3. L. Pachter, Models for transcript quantification from RNA-Seq. 1–28 (2011).
4. G. P. Wagner, K. Kin, V. J. Lynch, Measurement of mRNA abundance using RNA-seq data: RPKM measure is inconsistent among samples. *Theory Biosci.* (2012) https:/doi.org/10.1007/s12064-012-0162-3.
5. M. I. Cornwell, *et al.*, VIPER: Visualization Pipeline for RNA-seq, a Snakemake workflow for efficient and complete RNA-seq analysis. *BMC Bioinformatics* (2018) https:/doi.org/10.1186/s12859-018-2139-9.
6. A. Subramanian, *et al.*, Gene set enrichment analysis: A knowledge-based approach for interpreting genome-wide expression profiles. *Proc. Natl. Acad. Sci. U. S. A.* (2005) https:/doi.org/10.1073/pnas.0506580102.
7. H. Li, R. Durbin, Fast and accurate short read alignment with Burrows-Wheeler transform. *Bioinformatics* (2009) https:/doi.org/10.1093/bioinformatics/btp324.
8. C. Zang, *et al.*, A clustering approach for identification of enriched domains from histone modification ChIP-Seq data. *Bioinformatics* (2009) https:/doi.org/10.1093/bioinformatics/btp340.
9. G. Yu, L.-G. Wang, Q.-Y. He, ChIPseeker: an R/Bioconductor package for ChIP peak annotation, comparison and visualization. *Bioinformatics* **31**, 2382–2383 (2015).

10. M. Tarailo-Graovac, N. Chen, Using RepeatMasker to identify repetitive elements in genomic sequences. *Curr. Protoc. Bioinforma.* **Chapter 4**, Unit 4.10 (2009).

11. M. R. Lamprecht, D. M. Sabatini, A. E. Carpenter, CellProfiler: free, versatile software for automated biological image analysis. *Biotechniques* **42**, 71–5 (2007).

12. Y. Zhang, *et al.*, Integrated Analysis of Genetic Abnormalities of the Histone Lysine Methyltransferases in Prostate Cancer. *Med. Sci. Monit.* **25**, 193–239 (2019).

13. B. MacLean, *et al.*, Skyline: An open source document editor for creating and analyzing targeted proteomics experiments. *Bioinformatics* (2010) https:/doi.org/10.1093/bioinformatics/btq054.